THEORETICAL NOTES

NOTE 178

June 1973

X-RAY INDUCED PHOTOELECTRIC CURRENTS

by

Daniel F. Higgins

Mission Research Corporation

ABSTRACT

A simplified method for determining the x-ray induced, back-scattered photoelectric current from several different materials is discussed. The results of this simple method are compared with experimental data and more complicated calculations and reasonable agreement is obtained. Both the energy and angular dependence of the emitted photoelectrons are considered. A Planckian energy distribution for the incident x-ray pulse is assumed and the energy distribution of emitted photoelectrons is calculated for several materials. These energy distributions can be fitted by simple exponential functions over much of the energy range considered.

I. INTRODUCTION

In recent years system generated EMP has been recognized as a potential threat to systems located in the source region of a nuclear burst. Incident photons from the burst interact with the various materials of the system, producing electrons. The electrons move, creating currents and electromagnetic fields which, in turn, affect the electron motion. The complete problem is thus a very difficult one to address.

This report discusses just one small part of the overall problem -- namely, the backward emission of photoelectrons from a material illuminated by an x-ray pulse. X-ray induced emission is an especially important effect for exo-atmospheric systems illuminated by a high altitude burst since there is little or no intervening material to absorb the x-rays (see References 1, 2).

The attempt here has been to develop a simple model for describing the photoemission process. This model has been used to find analytic approximations of the emitted photocurrent for several different materials.

Certain features of the problem are difficult to treat in a simple manner, and more detailed calculations may well be needed for specific cases. However, it is believed that the model described here contains most of the relevant features of electron emission in the energy range being considered.

Much of the information in this report has been simply gathered from other sources and the reader interested in further study should consult the attached list of references. In particular, the author has borrowed freely from Longmire and Schaefer (References 3, 4).

The rest of this report is divided into several sections. Section II describes a simplistic method for estimating the total flux and energy dependence of an x-ray pulse from a hypothetical weapon. Section III discusses the electron emission process and gives estimates of the electron yield per incident photon. Energy and angular dependence of the emitted electrons are also discussed. Section IV folds an incident blackbody spectrum with the electron yield functions to obtain estimates of the net emitted photocurrents. Finally, Section V summarizes results, discusses limitations, and points out areas of future work.

II. DESCRIPTION OF THE INCIDENT X-RAY PULSE

Before considering the actual electron emission process, let us first review the characteristics of the incident x-ray pulse. The prime characteristics which one must consider are the total x-ray flux, the time history of the pulse, and the x-ray energy distribution.

The time integrated total x-ray energy flux (fluence) per unit area, ϕ, can be written as

$$\phi = \frac{f_x Y}{4\pi r^2} \quad , \tag{1}$$

where f_x = fractional x-ray yield
Y = total yield of weapon
r = distance from burst point to observer.

This expression does not include any x-ray attenuation due to material (e.g. air) between the burst point and the observer. The x-ray fractional yield, f_x, is typically fairly close to unity, say .7 or .8.[2] The total yield, Y, is most often expressed in tons.* Note that

$$1 \text{ ton} = 10^9 \text{ calories} = 4.1868 \times 10^9 \text{ joules} \quad . \tag{2}$$

The total x-ray fluence, ϕ, is most often given in units of calories/cm^2 where the energy has been integrated over the entire time history of the x-ray pulse. For example, consider the x-ray flux at a distance of 1000 km from a 1 MT burst with a fractional x-ray yield of .8. Then

* Of high explosive equivalent

$$\phi = \frac{(.8)(1.0 \times 10^6 \times 10^9)}{4\pi(10^8)^2} = 6.37 \times 10^{-3} \frac{\text{calories}}{\text{cm}^2} \quad (3)$$

For calculational purposes, it is most often assumed that the time-dependence of the x-ray pulse can be separated from the energy, position, and yield dependence; ie., it is assumed that the time-dependent flux is just

$$\phi(\vec{r}, Y, t) = \phi G(t) \quad , \quad (4)$$

where ϕ is just the fluence defined in Equation 1 and G(t) is a normalized time function with the property that

$$\int_0^\infty G(t)dt = 1 \quad . \quad (5)$$

In this case, t is actually a retarded time and t = 0 corresponds to the time the x-ray wavefront first reaches a given point in space.

The exact shape of the time function G(t) depends upon a variety of factors. Often, the waveform shape is not too critical and a simple triangular or $\sin^2$ waveform is used along with a specified pulse width at half-maximum. Pulse widths at half-maximum of the order of several tens of nanoseconds might be considered characteristic. One might also consider using the double exponential function

$$G(t) = \frac{ab}{b - a} \left(e^{-at} - e^{-bt}\right) \quad , \quad (6)$$

where a and b can be varied to describe the specific waveshape under consideration.

A third parameter of interest is the energy distribution of photons in the x-ray pulse. One should first note that a nuclear burst will emit numerous photons over a very wide energy range. While both x-rays and γ rays are electromagnetic quanta, it is conventional to separate them according to their origin in a nuclear burst. From widely known (and unclassified) properties of uranium fission, it is easily deduced that the temperature must be about 10 kev at the center of a nuclear explosion. As a result of this high temperature, both free and bound electrons emit energy in the form of electromagnetic radiation. The term x-ray refers to quanta emitted by these excited electrons. Gamma radiation, on the other hand, refers to those higher energy quanta emitted by nuclei left in excited states by fission or neutron reactions. Due to the difference in average photon energies between the x-ray and γ ray production processes, it is often convenient to call the energy range below 100 kev the x-ray range and that above 100 kev the γ ray range. We will use this energy cutoff definition in this report.

The emerging x-ray spectra of an actual weapon must be determined by detailed calculations or experiment. As a useful analytic approximation, x-ray radiation from the bomb debris is approximated by the Planckian or blackbody distribution function, S_b. The blackbody distribution for the number of photons of energy u (in kev) per unit energy interval is given by

$$S_b = Au^2\left[e^{u/u_T} - 1\right]^{-1} \quad , \tag{7}$$

where A is a normalization constant and u_T is the temperature, kT, of the distribution (in kev).

The normalization constant, A, can be defined by the requirement that

$$\int_0^\infty S_b(u)du = 1 \quad , \tag{8}$$

which gives

$$A = \left[2\zeta(3)u_T^{\,3}\right]^{-1} \quad , \tag{9}$$

where ζ is the Riemann zeta function. For reference, $\zeta(3) \simeq 1.202$.

A plot of the blackbody distribution for several temperatures is shown in Figure 1.

Note that as defined here, S_b is the photon number density spectrum as a function of photon energy. The energy density spectrum is obtained by just multiplying $S_b(u)$ by the energy u. Also, the average photon energy, $\bar{u}$, is just

$$\bar{u} = \int_0^\infty uS_b(u)du$$

$$= 3\,\frac{\zeta(4)}{\zeta(3)}\,u_T$$

$$\simeq 2.70\,u_T \quad . \tag{10}$$

One can compare this average energy with the peak of the spectrum which occurs at $u = u_p$. The value of u_p is given by setting

$$\frac{dS_b(u)}{du} = 0 \quad , \tag{11}$$

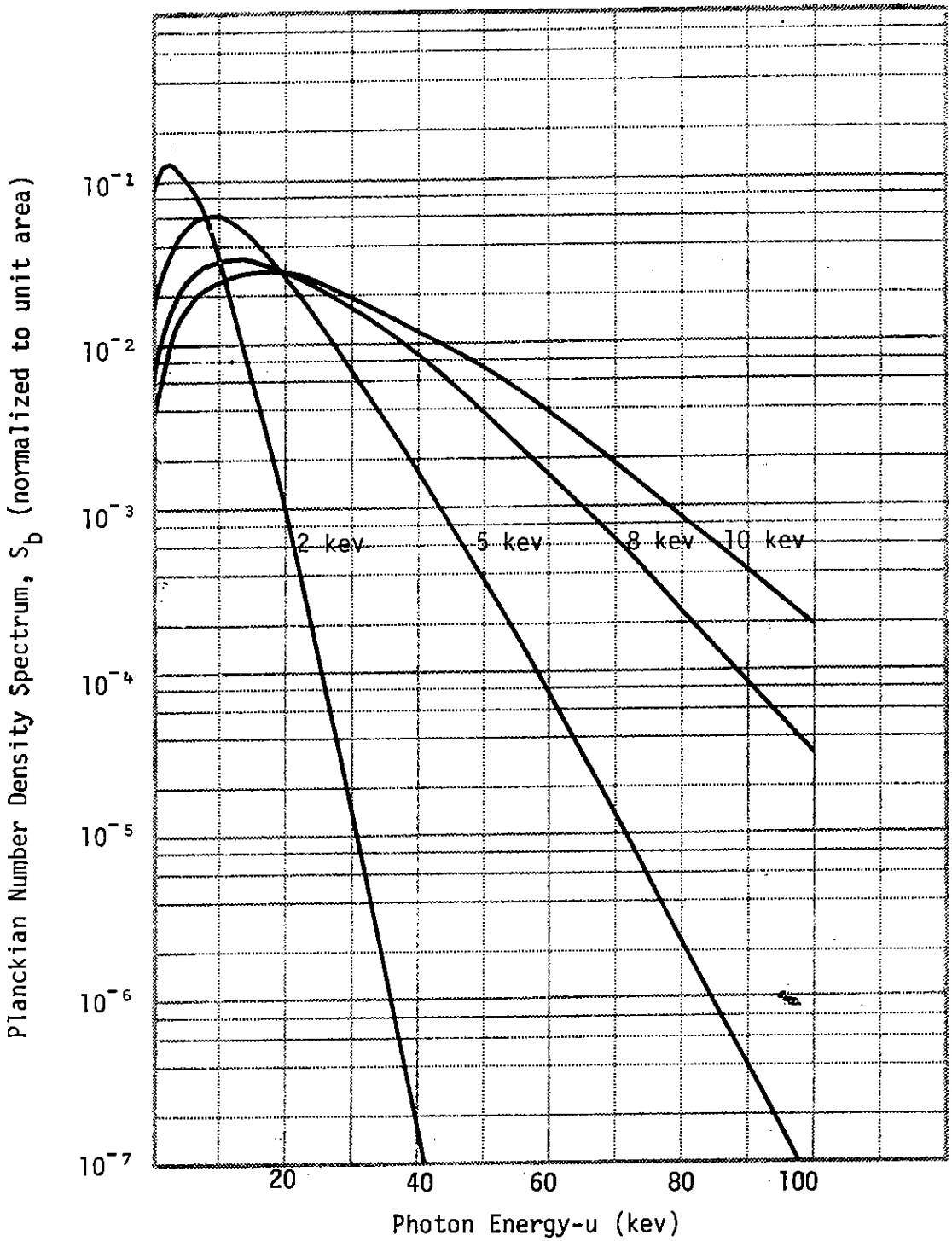

Figure 1: Planckian Number Density Spectrum as a Function of Photon Energy (photons/kev).

which gives

$$\left[2 - \frac{u_p}{u_T}\right] e^{u_p/u_T} - 2 = 0 \quad . \tag{12}$$

Solving this expression for u_p gives

$$u_p \simeq 1.6u_T \quad , \tag{13}$$

as the energy where the distribution peaks. Note that the peak energy is less than the average energy.[2]

Putting these various factors together one can write an expression for the differential energy flux

$$\frac{d^2\phi(\vec{r}, u, t)}{dudt} = \frac{\phi}{\bar{u}} uS_b(u)G(t) \quad . \tag{14}$$

This expression gives the energy incident per unit area per photon energy interval du per unit time interval dt. Note that

$$\phi = \int_o^\infty \int_o^\infty \frac{d^2\phi}{dudt} \, dudt \quad . \tag{15}$$

The time-independent flux, ϕ, can also just be written as

$$\phi = N_x \bar{u} \quad , \tag{16}$$

where $\bar{u}$ is defined in Equation 10 and N_x is the total number of photons incident per unit area. The differential number density flux is then just

$$\frac{d^2N_x}{dudt} = N_x S_b(u)G(t) = \frac{\phi}{\bar{u}} S_b(u)G(t) \quad . \tag{17}$$

For most cases of interest, the object being illuminated by the x-ray pulse is sufficiently distant from the source so that the x-ray wavefront looks like a plane wave (rather than a spherical wave). Thus, the incident x-ray pulse can, for most cases, be described as a plane wave with some direction of propagation along a radial line from the burst point and a differential flux spectrum as described in Equation 14. Such an incident x-ray pulse will be assumed throughout the rest of this report.

III. THE ELECTRON EMISSION PROCESS

A. Electron Emission - A Simple Model

When the incident x-ray pulse hits a slab of material, the photons interact with matter by a number of different processes so as to create free electrons. These processes include: (1) pair production, (2) Compton scattering, (3) the photoeffect, (4) the Auger effect (auto-ionization), and (5) secondary electron production from any of the four previous electron sources. X-rays have insufficient energy for pair production, and Compton scattering begins to become important only at the high energy end of the x-ray energy spectrum (i.e. at photon energies near 100 kev). Also, Compton electrons tend to be directed more in the forward direction and thus will not contribute proportionately to backward emission. On the other hand, Auger and secondary electrons tend to be numerous but have relatively low energy. Auger electrons result from outer-shell electrons falling into an inner electron shell and the energy difference being transferred to an outer-shell electron. Thus, Auger electron energies depend on the electron binding energies (which reach values of a few tens of kev only for high Z elements such as tantalum or gold). A vast number of secondary electrons may be produced with energies ranging from a few ev to perhaps several kev. These low energy secondaries may never reach the surface of the emitter and their effect is usually not considered very important even though it is only poorly understood.

This leaves the photoeffect as the prime source of electrons for photon energies in the range of about 5 to 100 kev. In the photoeffect the incident photon is completely absorbed, part of its energy going to free an atomic electron, the rest appearing as kinetic energy of

the free electron. The photoeffect is discussed more thoroughly in several references.[5,6]

Now let us consider the backward emission of electrons from a material illuminated by an incident x-ray pulse. For this simple model we will consider only photoelectric scattering of K-shell electrons. (A more complete discussion is given by Schaefer in Reference 3.) The geometry under consideration is shown in Figure 2. It is assumed that the material being illuminated is "thick" to electrons; i.e. the material is thicker than one electron range. Thus we need consider only those electrons "born" within one electron range of the material's surface. (For example, the mean range of a 100 kev electron in aluminum is about 9×10^{-3} gm/cm^2, or roughly 3.3×10^{-3} cm.) On the other hand, one should note that for most materials the incident photon beam is absorbed only slightly in distances comparable to the electron's range (e.g., the absorption coefficient for 100 kev photons in aluminum is 1.72×10^{-1}cm^2/g,

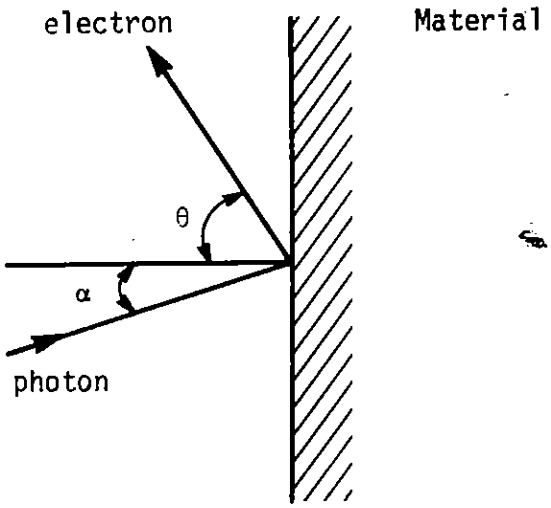

Figure 2: Electron Production Geometry

corresponding to a length of 2.16 cm). Thus, the photons are not appreciably attenuated in one electron range from the surface and thereby create a uniform electron source density in this region. This electron source density is equal to $\phi\mu/\cos\alpha$ where ϕ is the photon flux at the surface, μ is the photoelectric linear absorption coefficient, and α is the angle of incidence of the photon with respect to the normal (see Figure 2). The total number of electrons produced within one electron range, R_m, of the surface per unit area of exposed surface is then just

$$\text{number of electrons} = \frac{\phi\mu R_m}{\cos\alpha} \quad . \tag{18}$$

The photoelectric yield, Y_p, of the material (in units of electrons per incident photon) is then just given by

$$Y_p = \frac{f_p \mu R_m}{\cos\alpha} \quad , \tag{19}$$

where f_p is the fraction of electrons produced within one electron range of the surface that eventually escape from the surface.

The correct value of f_p is a somewhat difficult number to calculate accurately. In a simple model developed by Longmire (Reference 3), f_p was estimated to be 3/8, while Schaefer (Reference 4) obtained a value of 1/4, using slightly different assumptions. It should be noted that both of these references use a mean electron range, R_m, in Equation 18 rather than the total electron path length (extreme electron range). This is because the electron will suffer multiple collisions when traveling through the material. These collisions tend to randomize the initial electron angular distribution and result in a mean range along a given direction that is only a fraction of the total path length. (This fraction is roughly 1/2 for aluminum - see Reference 4,7.)

Now consider the angular dependence of the emitted photoelectrons. A simple method is to just compare the electrons to randomly moving particles escaping through a small hole in a box. If expressed in terms of electrons per steradian the familiar cosine distribution appears. In terms of θ, the differential yield just becomes

$$\frac{dY}{d\theta} = \frac{2f_p \mu R_m}{\cos \alpha} \sin \theta \cos \theta \quad , \tag{20}$$

where we have normalized $dY/d\theta$ such that

$$Y = \int_{\theta=0}^{\pi} \frac{dY}{d\theta} \, d\theta \quad . \tag{21}$$

This simple angular dependence agrees rather well with both more complex calculations and experimental results.[8,9] It thus appears that the assumption of randomizing multiple scattering of the electrons is justified.

Next, let us consider the energy dependence of the emitted photoelectrons. For an incident photon of given energy, a photoelectron has a kinetic energy at birth given by the difference between the photon's energy and the binding energy of the electron shell in question. For aluminum, the binding energy of the K-shell is 1.56 kev and thus photons with energies far above the K-edge create electrons of approximately equal energy.

These photoelectrons, however, must travel some distance through the material in which they were created before they escape. These electrons lose energy as they travel through the material due to ionization. This energy loss is described by some effective stopping power, dE/dr. Thus, electrons born further from the surface will have less energy when they finally escape than electrons born nearer the surface.

Keeping these thoughts in mind, one can write a differential energy yield, dY/dE where E refers to the kinetic energy of the electron. (For the energies being considered the use of classical rather than

relativistic mechanics is sufficiently accurate for our purposes.) Using Equation 19, the differential energy yield becomes

$$\frac{dY}{dE} = \frac{f_p \mu}{\cos \alpha} \frac{dR_m}{dE} = \frac{f_p \mu}{\cos \alpha} \left(\frac{dE}{dr}\right)^{-1} \quad . \tag{22}$$

In this case, the normalization requirement is

$$Y = \int_0^{u-E_i} \frac{dY}{dE} \, dE \quad , \tag{23}$$

where E_i is the binding energy of the i^{th} electron shell. Thus the integration is over all electron energies from zero to the initial energy $(u - E_i)$. [Remember that u is the energy of the incident photon.]

The simple result in Equation 22 makes it possible to estimate the energy dependence of the emitted photoelectrons from a knowledge of the electron range as a function of energy. It is known that the range varies roughly as E^2 for a number of materials. Thus, from Equation 21, the differential energy yield should vary as E. This approximate linear energy variation has been observed both in Monte Carlo calculations and experimental results (References 4, 8, 10). Thus, the use of a roughly triangular energy spectrum appears justified as long as photon energies are not too near absorption edges and the Compton contribution can be ignored.

B. Comparison of Photoelectric Yield Results

As mentioned previously, the simple photoelectric yield model discussed here gives reasonably good results with respect to the electron energy distribution and angular dependence. Another question, not yet considered, is the accuracy of the total yield predicted by such a model. As noted, there is some question as to what value should be used for fraction f_p, defined in Equation 18. To answer this question, one needs to compare the photoelectric yields from a number of different sources.

Such a comparison for the backward photoelectric yield from aluminum is shown in Figure 3. It is readily seen that there is some disagreement between the various sources listed. Schaefer's model (Reference 4) seems to agree fairly well with experimental data, indicating that an f_p of 1/4 should be used for aluminum. Although not shown in Figure 3, it should also be noted that the experimental work of Bradford (Reference 9) and the calculations of Chadsey (Reference 8) are consistent with each other within roughly 20-30% and appear to agree with the estimates of Schaefer shown in Figure 3.

One of the yield curves plotted in Figure 3 is taken from a Sandia report (Reference 12) by Dellin and MacCallum. This report is a handbook giving predictions of the photoelectric and Compton currents under equilibrium conditions in unbounded media. Predictions for currents in 24 elements and 13 compounds are given and a model for calculating interface currents is discussed. The authors claim this interface model gives a reasonable upper limit on the backward directed current and the comparison shown in Figure 3 tends to verify this. Thus, this reference is a particularly useful source of information since a variety of materials are treated. It does appear that the yields are about a factor of two above experimental measurements.

Keeping these limitations in mind, Reference 12 was used to prepare Table 1, which gives approximate analytic fits to electron yield curves for various materials. The yields can be fitted fairly well by the simple function

$$Y = A\left(\frac{u}{u_o}\right)^{-n_1} \quad , \tag{24}$$

where u is the incident photon energy and A, u_o, and n_1 are given for various materials in Table 1. For the low Z materials these fits are fairly accurate from about 5 to 100 kev. For high Z elements the K-shell

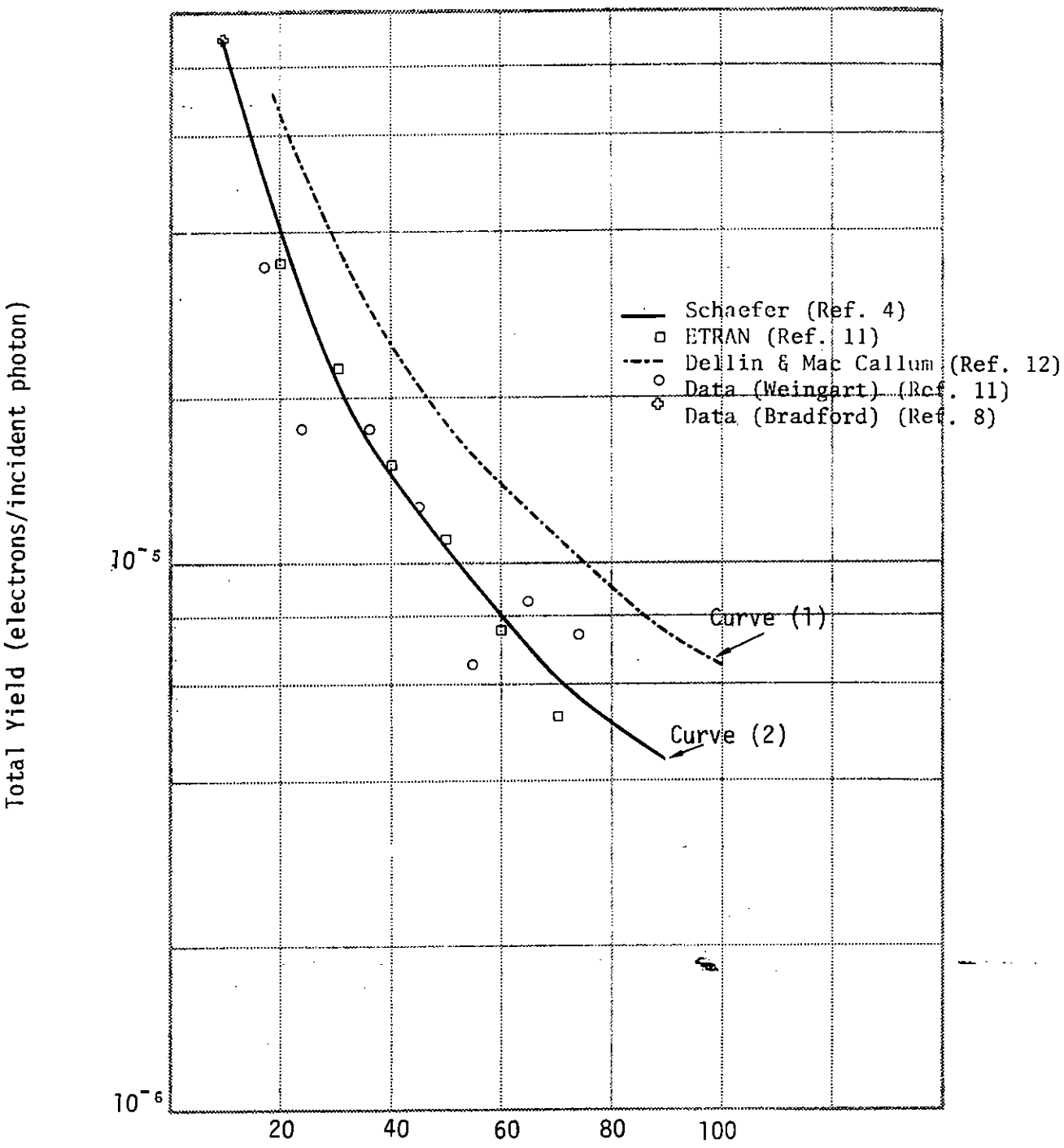

Figure 3: Comparison of Backscattered Total Yield Estimates for Aluminum

absorption edge occurs at higher energies. The absorption edge causes sharp bends in the electron yield function. Thus, in Table 1, the yield function for tantalum is fit by different functions over two different energy ranges.

Similarly, using the normalization requirement of Equation 22, the differential yields with respect to energy can be fit by the expression

$$\frac{dY}{dE} = B \frac{E^{n_2}}{u^{n_3}} \qquad \text{where } E < u - E_i \quad . \qquad (25)$$

The parameters B, n_2, and n_3 are given for various materials in Table 2.

In compiling this table we have assumed that the differential yield varies linearly with electron energy (i.e. $n_2 = 1.0$). It is possible to use Equation 21 and an accurate fit to the slope of the stopping power (see Reference 4). For the low Z materials considered, such a process gives an n_2 value slightly less than unity (roughly .7 to .8). However, experimental and Monte Carlo calculation (References 4,10) indicate that n_2 should be slightly greater than 1. Thus, a simple linear slope appears more accurate than actually using an expression for the stopping power in Equation 21.

Note that in Tables 1 and 2 there are two sets of fit parameters for aluminum. The first is a direct fit of the information in Reference 17. The second is adjusted to fit the experimental data shown in Figure 3. Thus, the first fit parameters indicate a worse case estimate, while the second set are a less conservative estimate. The appropriate curves are indicated in Figure 3.

Material	u_o (kev)	A	n_1
Aluminum (1)	10	1.55×10^{-3}	1.35
Aluminum (2)	10	8.61×10^{-4}	1.35
Silicon Dioxide	10	1.0×10^{-3}	1.43
Polyvinyl Chloride (PVC)	10	1.6×10^{-3}	1.23
Copper	10	9.9×10^{-3}	.92
Tantalum (15-60 kev)	15	2.0×10^{-2}	.72
(60-200 kev)	60	7.4×10^{-3}	-.37

(1) and (2) refer to curves in Figure 3.

Table 1. Analytic fits of the total electron yield - $Y = A\left(\frac{u}{u_o}\right)^{-n_1}$ for 5 kev < u < 100 kev (Y in units of electrons/incident photon).

Material	B	n_2	n_3
Aluminum (1)	.069	1.0	3.35
Aluminum (2)	.038	1.0	3.35
Silicon Dioxide	.054	1.0	3.43
Polyvinyl Chloride	.054	1.0	3.23
Copper	.165	1.0	2.92

(1) and (2) refer to curves in Figure 3.

Table 2. Analytic fits to the differential energy yield- $dY/dE = BE^{n_2}/u^{n_3}$ for $E \leq u$, 5 < u < 100 kev (dY/dE in units of electrons/photon-kev, E, u in kev).

IV. PHOTOELECTRIC CURRENT FROM AN X-RAY PULSE WITH A PLANCKIAN ENERGY DISTRIBUTION

In the previous two sections simplified means of describing both the incident x-ray pulse and the electron yield per incident photon have been developed. In this section, these two processes will be folded together to obtain a description of the net photoelectric current density backscattered by various materials.

The photoelectric current, $j(E, t, \theta)$, written in terms of electrons per unit area per unit energy (E) per unit time (t) per unit angle (θ) can be written

$$j(E, t, \theta) = \int_u \frac{d^2N_x}{dudt} \frac{d^2Y}{dEd\theta} du \quad . \tag{26}$$

Note that in general the incident differential flux also depends on the angle of incidence, α, (see Figure 2). The photoelectric current then must also include an integral over all possible angles of incidence, i.e.,

$$j(E, t, \theta) = \int_\alpha \int_u \frac{d^2N_x(u, t, \alpha)}{dudt} \cos \alpha \frac{d^2Y}{dEd\theta} du d\alpha. \tag{27}$$

The cos α term in the integrand just gives the projected area of the unit surface area being considered. Note, however, that the

differential yield (Equation 20) has a cos α term in the denominator which will just cancel the same term in the integrand of Equation 27. Since in the case under consideration we expect all the incident photons to be roughly parallel (i.e. the distribution over α is a delta function), then the angular dependence with respect to α disappears. Another way of thinking about this is to note that as the angle of incidence increases the projected surface area from which electrons are emitted decreases as $[\cos \alpha]^{-1}$. On the other hand, remembering that all escaping electrons must be born within one electron range from the surface, it is easily seen that the x-ray path length through this electron birth region increases with angle as $[\cos \alpha]$. Since the number of electrons produced varies linearly with the x-ray path length, the two angular effects cancel. This indicates the photocurrent leaving the material is a function only of the total emitting area and not the angle of incidence. (This independence breaks down for angles of incidence near $\pi/2$.)

Using Equations 14, 20, 22, and 25 in Equation 27 gives the photoelectric current as

$$j(E, t, \theta) = 2N_x G(t) \sin\theta \cos\theta \int_{u=E+E_i}^{u_{max}} S_b(u) f_p \mu \left(\frac{dE}{dr}\right)^{-1} du$$

$$= 2N_x BG(t) \sin\theta \cos\theta \int_{u=E+E_i}^{u_{max}} \left(\frac{S_b(u)}{u^{n_3}}\right) E^{n_2} du \qquad (28)$$

Since the integral involves only energy terms, it is convenient to simplify $j(E, t, \theta)$ by integrating over t and θ. Thus

$$j(E) = N_x B E^{n_2} \int_{u=E+E_i}^{u_{max}} \frac{S_b(u)}{u^{n_3}}\, du \quad . \tag{29}$$

Note that the limits of integration reflect the fact that it takes a photon of at least energy $E + E_i$ to produce an electron of energy E. If we explicitly write out $S_b(u)$, j(E) becomes

$$j(E) = \frac{N_x B E^{n_2}}{2\zeta(3) u_T^{\,3}} \int_{u=E+E_i}^{u_{max}} \frac{u^{2-n_3}}{[e^{u/u_T} - 1]}\, du \quad . \tag{30}$$

The integral in Equation 30 cannot, in general, be evaluated analytically. Thus, we have numerically carried out the integration for several materials and blackbody temperatures. The resulting spectra are shown in Figures 4-8. One should note that the integral tends to diverge as the photon energy u becomes small. This is due to the fact that the electron yield functions used are not accurate at low energies. To avoid such divergence problem , the integral is numerically evaluated from the upper limit backwards. It is assumed that u_{max} equals 100 kev.

It is readily seen that the curves in Figures 4-8 are roughly linear on a log-linear plot. Thus, over a substantial part of the energy range, the current, j(E) can be approximated by an exponential

$$j(E) = N_x C e^{-n_4 E} \quad . \tag{31}$$

The parameters C and n_4 are listed in Table 3 as a function of material and blackbody temperature.

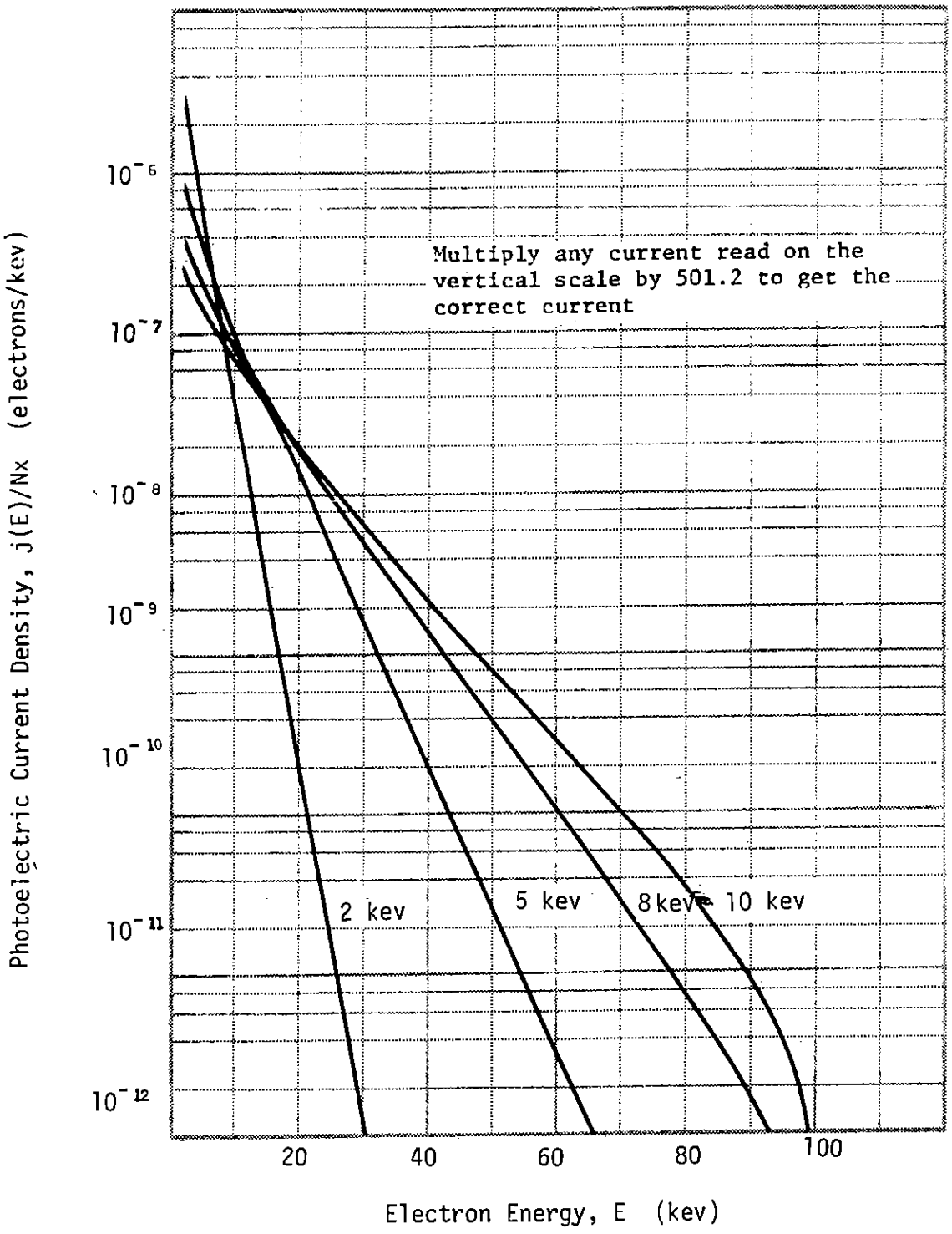

Figure 4: Photoelectric Current as a Function of Electron Energy - Aluminum (1)

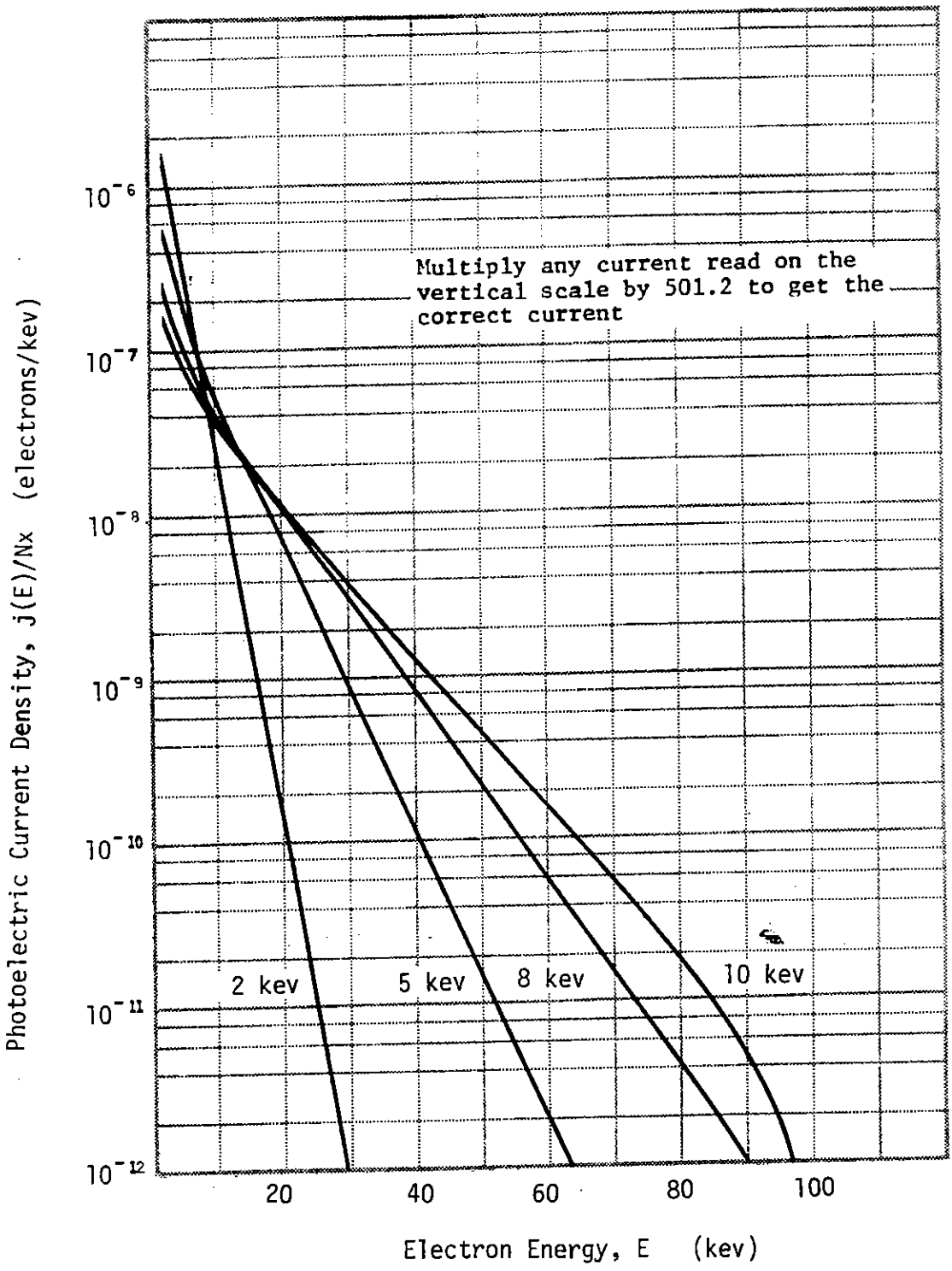

Figure 5: Photoelectric Current as a Function of Electron Energy - Aluminum (2)

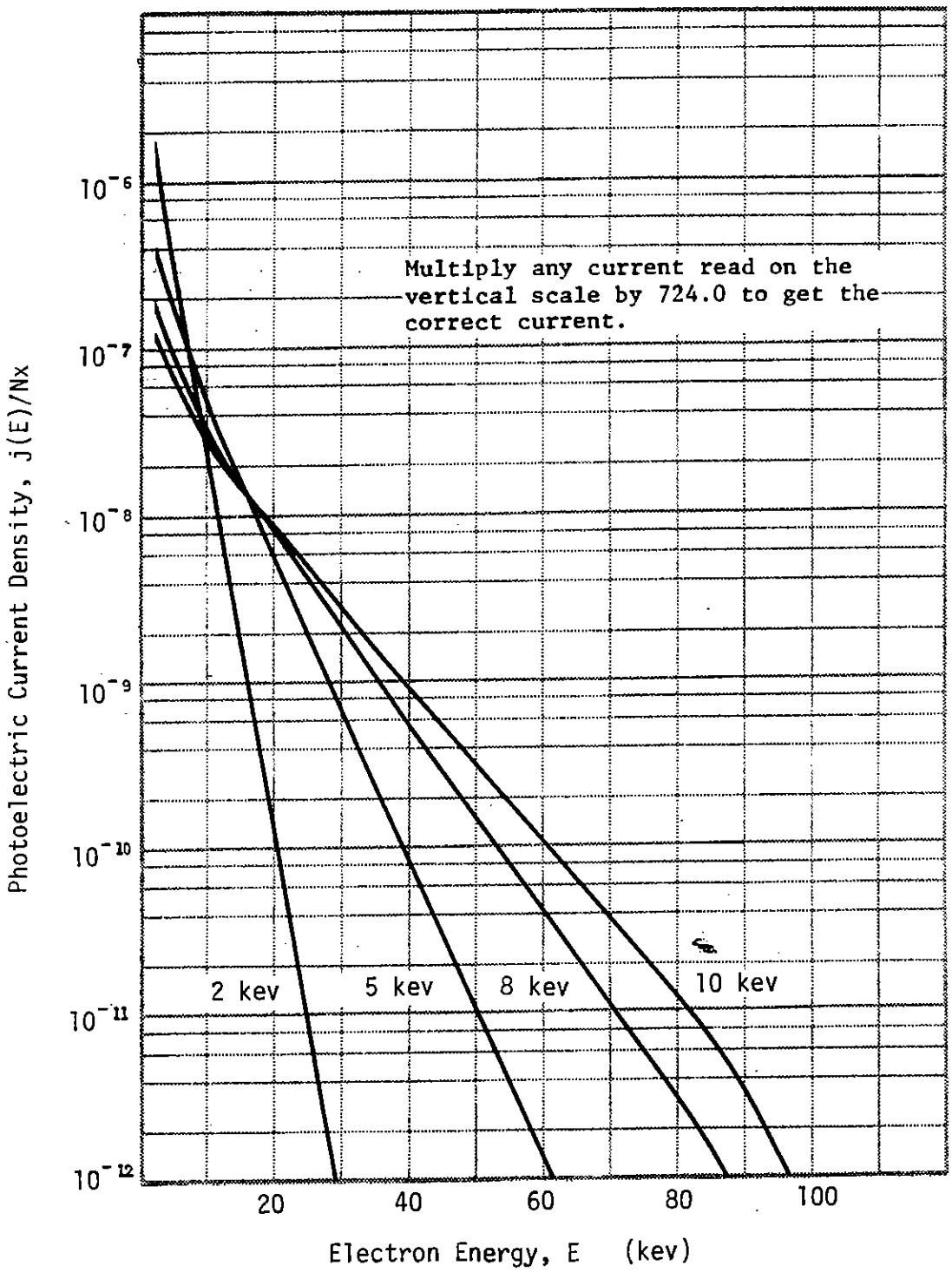

Figure 6: Photoelectric Current as a Function of Electron Energy - Silicon Dioxide

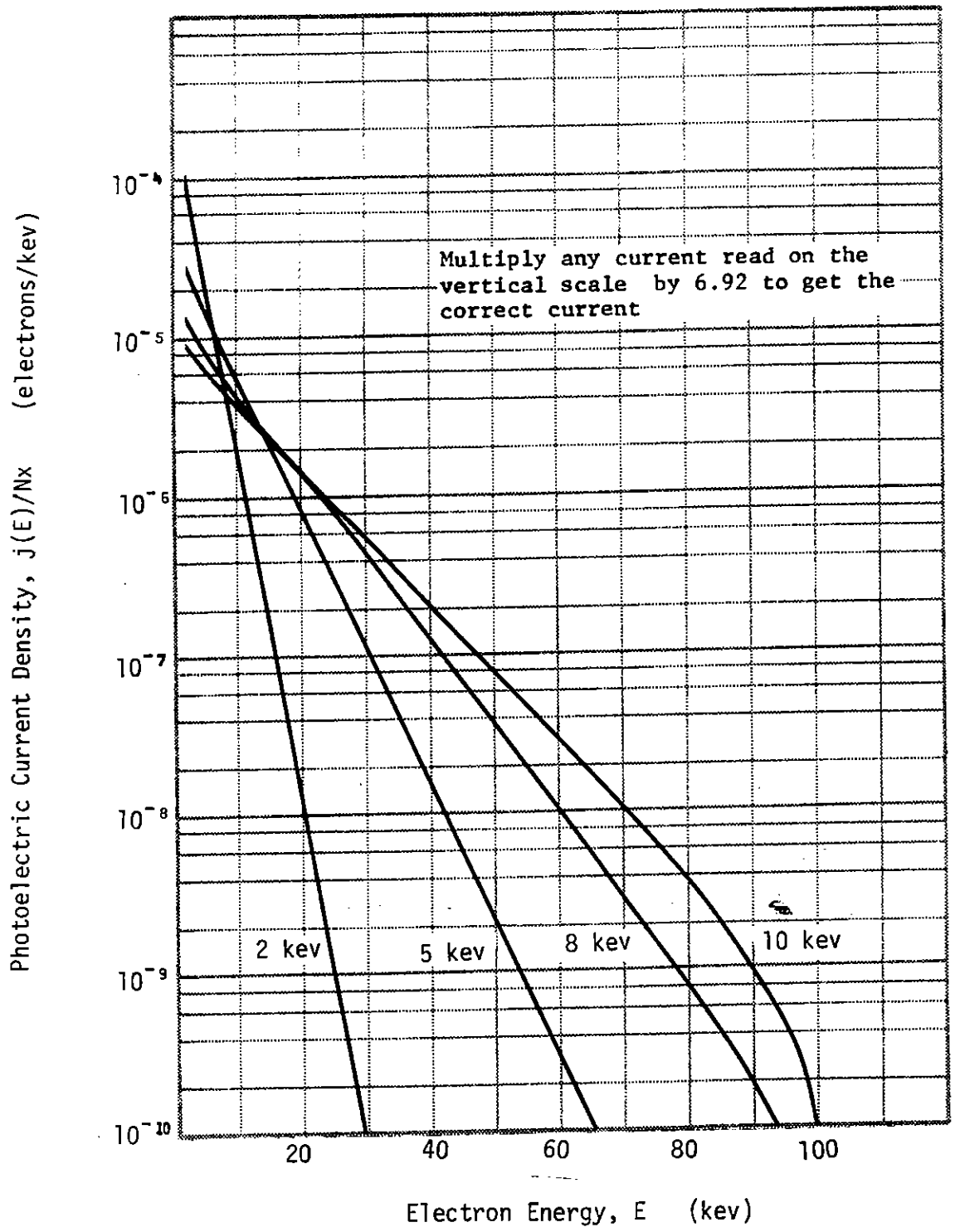

Figure 7: Photoelectric Current as a Function of Electron Energy - Copper

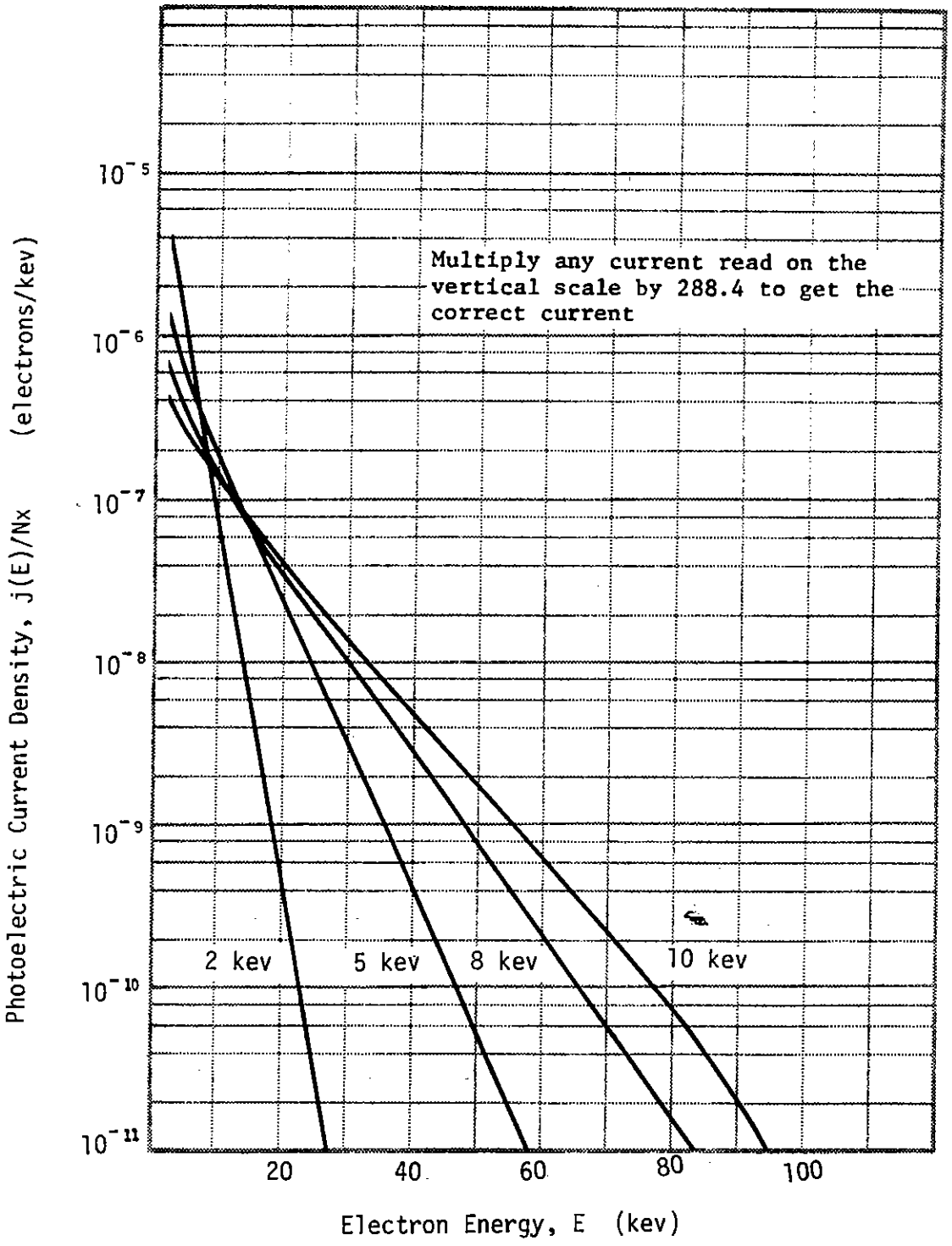

Figure 8: Photoelectric Current as a Function of Electron Energy - Polyvinyl Chloride

Material	Blackbody Temperature (kev)	C	n_4
Aluminum (1)	2	2.85×10^{-3}	.52
	5	3.87×10^{-4}	.21
	8	1.29×10^{-4}	.13
	10	9.22×10^{-5}	.11
Aluminum (2)	2	1.69×10^{-3}	.52
	5	2.19×10^{-4}	.21
	8	6.71×10^{-5}	.13
	10	5.06×10^{-5}	.11
PVC	2	2.84×10^{-3}	.51
	5	3.83×10^{-4}	.20
	8	1.46×10^{-4}	.13
	10	9.94×10^{-5}	.11
Silicon Dioxide	2	2.24×10^{-3}	.54
	5	2.39×10^{-4}	.21
	8	7.96×10^{-5}	.13
	10	5.21×10^{-5}	.11
Copper	2	1.61×10^{-3}	.50
	5	2.43×10^{-4}	.19
	8	1.01×10^{-4}	.12
	10	8.99×10^{-5}	.10

Table 4. Analytic Fit Coefficients for Backward Directed Photocurrents- $j(E) = N_x C e^{-n_4 E}$ where E is the electron's kinetic energy in kev.

It should be noted that these simple exponential functions tend to become inaccurate at low energies ($\lesssim 10$ kev) and at the higher end of the energy range ($\gtrsim 80$ kev). However, these simple fits are probably reasonable starting points for a number of electromagnetic field calculations requiring some estimate of the emitted current density.

An interesting observation that might be made from Table 3 is that the factor n_4 seems to depend mainly on the blackbody temperature, while C depends on both the material and the blackbody temperature.

V. CONCLUSIONS

From the previous sections, we have seen that it is possible to develop simple equations describing the backward emission of photoelectrons from the surface of several different materials. It is assumed that the time, angular, and energy dependence are all independent so that the emitted current can be written as a product of three distribution functions. An examination of existing data and more precise calculations indicates that this separation is reasonable.

Another useful simplification is the fact that the emitted current is approximately independent of the x-ray angle of incidence. Thus, the total emitted current depends only on the total exposed area. A time-dependent current for various geometries can be written by simply "turning on" the photocurrent at various places on the surface at the appropriate retarded time.

The model described here has some limitations which may, in certain cases, be relatively important. First of all, no attempt has been made to describe the numerous secondary electrons or the Auger electrons that may be quite numerous at energies near the absorption edges of the material in question. (This is the reason why no energy dependent yields or photocurrents were given for tantalum on Tables 2 and 3). At the high energy end of the spectrum Compton electrons have been ignored. If Compton electrons are important, the simple linear dependence of dY/dE with electron energy is no longer valid. Also, it has been noted that there is some uncertainty in the value of the total electron yield, Y.

With sufficient effort, some of these limitations may be removed at the expense of creating a more complicated electron emission model. The model described here is probably accurate at least within a factor of two and should be useful as the starting point for a number of electromagnetic calculations. Specific cases, however, might require a more accurate treatment.

REFERENCES

1. Capt. Carl E. Baum, Interaction Note 76, "Electromagnetic Pulse Interaction Close to Nuclear Bursts and Associated EMP Environment Specification," July 1971.

2. Carl E. Baum, Sensor and Simulation Note 156, "A Technique for Simulating the System Generated Electromagnetic Pulse Resulting from an Exoatmospheric Nuclear Weapon Radiation Environment," September 1972.

3. C. L. Longmire, Theoretical Note 124, "External System Generated EMP on Some Types of Satellite Structures," August 1971.

4. R. R. Schaefer, "Simple Model of Soft X-ray Photoemission," J. Appl. Phys., Vol. 44, No. 1, January 1973. (Also R and D Associates report RDA-TR-036-DNA November 1971.)

5. W. Heitler, The Quantum Theory of Radiation, pp. 204-211, Third Edition (1954), Oxford University Press, London.

6. H. Bethe and J. Askins. "Passage of Radiation Through Matter," in Experimental Nuclear Physics, edited by E. Segre.

7. C. L. Longmire, Unpublished memo, "Energy Loss of Electrons," Mission Research Corporation, July 1972.

8. J. C. Garth and W. L. Chadsey, "Poem Code Calculations of X-ray Photoemission," DNA IEMP Symposium, San Diego, California, February 1973.

9. J. N. Bradford, "Absolute Yields of X-ray Induced Photoemissions from Metals," IEEE Trans. Nuc. Sci. N5-20, December 1972 (as reported in Reference 9).

10. Capt. C. R. Hale (editor), Theoretical Note 121, "Review of Internal EMP Technology," April 1971.

REFERENCES (continued)

11. F. R. Kovar, "Comparison of ETRAN Calculations With Experiment," DNA IEMP Symposium, San Diego, California, February 1973.

12. T. A. Dellin and C. J. MacCallum, "A Handbook of Photo-Compton Current Data." SCR-RR-720086 December 1972.